On diffuse-interface modeling of high-pressure transcritical fuel sprays

By L. Jofre, J. Urzay, A. Mani AND P. Moin

1. Motivation and objectives

At subcritical pressures, atomization devices in chemical-propulsion systems must ensure proper rupture of the liquid volume through aerodynamic shearing and homogeneous dispersion of the liquid droplets in the combustion chamber. The gas environment in the combustor is typically hot as a result of the heat released by chemical reactions, with part of its enthalpy being employed in vaporizing the liquid phase. The resulting vapor mixes and burns with the ambient gas in the combustor. Several studies have tackled the combustion dynamics of sprays and the resulting flame structures at low pressures (e.g. see Sánchez *et al.* (2015) and references therein). Conversely, not much is known about high-pressure sprays, partly due to the challenges associated with experimental diagnostics and analytical modeling for such extreme conditions.

High-pressure combustion of liquid propellants is of relevance for a number of propulsion systems. However, injection configurations tend to be specific to the practical application under consideration. For instance, in liquid rocket engines, cryogenic liquid oxidizer is injected along with gaseous fuel coflows at extremely high pressures. In these conditions, the coflow is supercritical and the liquid oxidizer stream promptly reaches the same thermodynamic conditions upon completion of a short heating period that increases its temperature a few degrees up to the critical value. Downstream from the injector, in the supercritical mixture, the latent heat of vaporization vanishes and there is virtually no surface tension that prevents rupture of the liquid core and diffusive mixing with the gas environment (Mayer *et al.* 2013). Although supercritical phenomena have been studied extensively in rocket engines because of the high pressures involved (Sirignano & Delplanque 1999; Yang 2010), they have also been observed in recent experiments in high-pressure reciprocating engines (Dahms *et al.* 2013). Supercritical dynamics is also becoming increasingly relevant in gas-turbine engines given the current trends that gear design towards higher compression ratios to increase efficiency and performance (Mongia 2013), although much less is known of these systems in high-pressure operation regimes.

In gas-turbine engines, the hydrocarbon liquid fuel is typically injected at ambient temperatures, while the oxidizer is provided by the air bled from the compressor. At pressures below the critical value, subcritical atomization dominates with primary and secondary stages taking place downstream from the injector (Lasheras & Hopfinger 2000). Conversely, supercritical dynamics occur in the combustor at pressures above the critical value for the mixture. Since the liquid fuel is seldom preheated to supercritical temperatures before injection, and a temperature increment of order $\Delta T = 400 - 500$ K is typically required to reach critical values in hydrocarbons, the presence of both subcritical and supercritical conditions near the injector in the combustion chamber seems warranted. This requires simultaneous consideration of the liquid phase near the orifice, which may contain droplets and ligaments influenced by non-zero surface-tension forces, in addition to subcritical vapors and supercritical phases downstream, as described be-

low. In principle, the analytical treatment of the multiphase mixture is facilitated by the larger thickness of the resulting interfaces at such high pressures (Dahms & Oefelein 2013). The objective would therefore be to describe the transcritical atomization problem with a single-fluid, multi-phase formulation that allows for continuum treatment of the multi-component mixture in the vicinity of the critical point while accounting for finite surface-tension effects and molecular diffusion across interfaces and mixing layers.

In this report, a preliminary investigation of high-pressure spray phenomena is performed. The report is organized as follows. In Section 2, focus is on the characteristic scales and resulting atomization regimes. A review of the diffuse-interface approach is made in Section 3. Finally, conclusions and future work are discussed in Section 4.

2. Characteristic high-pressure atomization regimes

Consider the simple flow configuration depicted in Figure 1, in which a liquid-fuel jet coflowing with a hot air stream discharges in a combustor at pressure P_0. Of particular relevance for the analysis is the characterization of the critical pressure and temperature of both streams, denoted here by the subindex $_c$. For instance, while $T_{c,A} \sim 126$ K and $P_{c,A} \sim 34$ atm for air, typical critical values for aviation fuels are $T_{c,\mathrm{F}} \sim 650-800$ K and $P_{c,\mathrm{F}} = 18-30$ atm (Yu & Eser 1995). While usual coflow temperatures $T_A \sim 1000-1200$ K are above the critical temperature of air, in aviation fuels a heat-up period exists in which the temperature of the fuel increases from the ambient injection value $T_\mathrm{F} = 300$ K to the critical temperature $T_{c,\mathrm{F}}$, with the isotherm $T = T_{c,\mathrm{F}}$ indicating critical conditions in the liquid; e.g. dashed lines in Figure 1(b,c). Transcritical conditions therefore arise near the injector when the liquid is injected at supercritical pressures, $P_0 > P_{c,\mathrm{F}}$. This is in contrast with liquid rocket engines, in which the liquid oxidizer only requires a small temperature increment of $20-30$ K to achieve supercritical conditions, which represents an extremely short heat-up period of not much practical relevance.

In connection with practical applications, attention is given here to turbulent fuel jets at high Reynolds numbers, $\mathrm{Re}_\mathrm{F} = U_\mathrm{F} R/\nu_\mathrm{F} \gg 1$, with U_F and ν_F the corresponding injection velocity and kinematic viscosity, respectively. The aerodynamic Weber number, $\mathrm{We} = \rho_A U_A R^2/\sigma$, with $U_A \sim U_\mathrm{F}$ the coflow velocity, is typically large near transcritical conditions because of the associated small values of the surface tension.

At high Weber and Reynolds numbers, and for ambient pressures below the critical pressure of the liquid component, subcritical atomization processes involve primary break-up of the liquid column in ligaments. In a secondary atomization stage, the ligaments break up and a spray of droplets is formed. This regime is depicted in Figure 1(a), where L_a denotes the liquid-core length. In particular, L_a can be estimated as $L_a \sim (12R/\sqrt{M})[1-\sqrt{\rho_\mathrm{A}/(\rho_\mathrm{F} M)}]^{-1}$ in the high Weber-number limit (Lasheras & Hopfinger 2000), with $M = \rho_\mathrm{A} U_\mathrm{A}^2/\rho_\mathrm{F} U_\mathrm{F}^2$ being a momentum ratio that attains typical values of order $10-20$ in air-blast atomization, in which the excess of kinetic energy in the air stream is essential for the aerodynamic shearing of the liquid. Since $\rho_\mathrm{F}/\rho_\mathrm{A} \sim 10^2-10^3$ at typical subcritical pressures, the liquid-core length is proportional to the orifice diameter in air-blast atomization, $L_a \gtrsim 2R$. Conversely, the jet breakup may become considerably delayed $L_a \gg 2R$ in the presence of slow coflows. In either case, the droplets resulting from atomization are dispersed by the underlying turbulent flow, first giving rise to zones in which the corresponding mass-loading ratio is large compared to unity, with the coflowing gas being locally cooled due to the lower temperature of the dense droplet cloud. This zone is followed by an increasingly diluted spray where the heat transferred

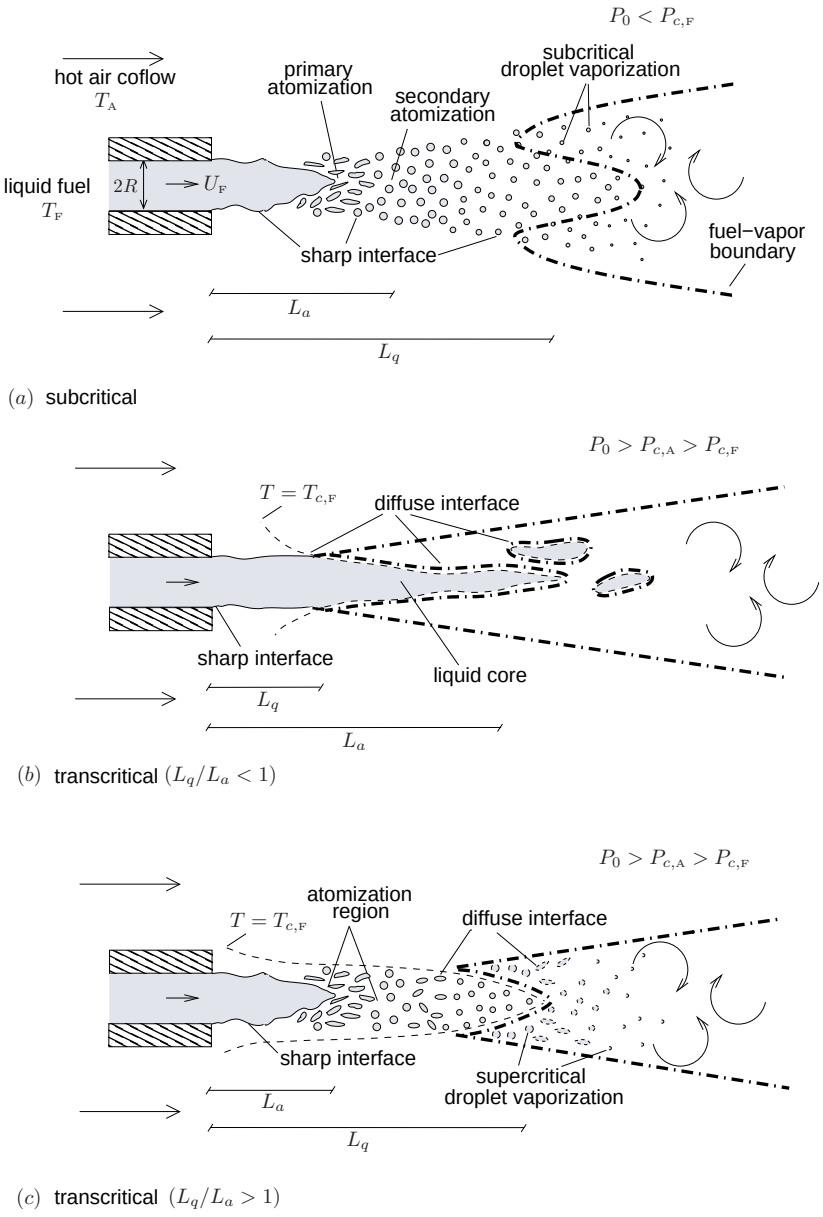

(*a*) subcritical

(*b*) transcritical ($L_q/L_a < 1$)

(*c*) transcritical ($L_q/L_a > 1$)

FIGURE 1. Atomization regimes at (a) low pressures or subcritical conditions, (b) high pressures with transcritical conditions reached prior to atomization of the liquid core, and (c) high pressures with transcritical conditions reached after atomization of the liquid core. The symbols are defined in the main text.

by the coflowing gas to the liquid enables the temperature of the droplets to increase to values near the boiling point at a streamwise distance L_q that corresponds to the thermal-entrance length of the spray. Droplet vaporization starts in this region and gives rise to a fuel-vapor cloud that ultimately burns with the ambient oxidizer. It is important to point out that the liquid-gas interface, which spans less than a single mean free path,

remains sharp at subcritical pressures and its exact resolution is untenable. Therefore, two-fluid formulations coupled through appropriate boundary conditions at the interfaces near the orifice (Gorokhovski & Herrmann 2008), along with multi-continua conservation equations or Lagrangian descriptions for the dilute spray downstream (Sirignano 2010), represent natural analytical representations of this regime.

In contradistinction, the atomization of liquids discharging in ambients at fully supercritical pressures, $P_0 > P_{c,\mathrm{A}} > P_{c,\mathrm{F}}$, is fundamentally different, as depicted in Figure 1(b,c). In particular, the relative importance of the atomization mechanisms described above diminishes when the temperature of the liquid fuel reaches the corresponding critical value $T_{c,\mathrm{F}}$ as a result of the heat transferred from the coflowing air. For aviation fuels, the corresponding change of temperature is of order unity, $(T_{c,\mathrm{F}} - T_{\mathrm{F}})/T_{\mathrm{F}} \sim 1.0 - 1.7$, which is achieved at characteristic streamwise distances of the same order as the thermal-entrance length L_q. In single-phase flows at high Reynolds numbers, L_q is of the same order as the jet diameter, $L_q/2R = O(1)$. In the entrance region, the surface tension σ undergoes decrements of order unity with respect to its nominal subcritical value σ_0, while attaining vanishing values downstream from the transcritical isotherm $T = T_{c,\mathrm{F}}$. In this way, the non-zero surface tension leads to finite Weber-number effects upstream from the transcritical isotherm. Note that the use of intermediate pressures, $P_{c,\mathrm{A}} > P_0 > P_{c,\mathrm{F}}$, leads to a more complicated structure in which subcritical conditions prevail everywhere in the air stream while the fuel jet undergoes transition to supercritical vapor.

The ratio L_q/L_a, which corresponds to the competition between thermalization and atomization of the fuel jet, represents an important parameter of the problem (Banuti & Hannemann 2014) that is specific to the operating conditions and dictates whether the critical conditions occur prior to break-up (i.e. $L_q/L_a < 1$) or after break-up of the liquid jet (i.e. $L_q/L_a > 1$). In the atomization regime resulting from values $L_q/L_a < 1$, which is depicted in Figure 1(b), instabilities may occur at the fuel-air interface where it is sharp near the orifice and $\sigma \sim \sigma_0$, but an incipiently vanishing surface tension makes the interface to become increasingly thicker as the critical temperature is approached while the mean free path decreases. As a result, the dominant process far downstream from the transcritical isotherm departs from classic atomization driven by aerodynamic shear and becomes turbulent mixing between supercritical vapors of fuel and oxidizer (Segal & Polikhov 2008). The resulting structure is sketched in Figure 2. On the contrary, for $L_q/L_a > 1$, the liquid core upstream from the transcritical isotherm undergoes atomization driven by finite surface-tension effects resulting in droplets that vaporize in a supercritical environment downstream from the transcritical isotherm, thereby generating a cloud of supercritical vapor of fuel as depicted in Figure 1(c). Because of the relatively larger thermal-entrance length required to heat up heavy hydrocarbon fuels, the regime $L_q/L_a > 1$ is most prone to occur in gas turbines or internal-combustion engines (e.g. see recent experimental investigations by Crua *et al.* (2015)), while the regime $L_q/L_a < 1$ of prompt transition to supercritical dynamics in absence of droplets is often observed in rocket engines because of the extremely high combustor pressures and the near-critical injection temperatures utilized for the liquid oxygen (e.g. see experimental images reported in Mayer *et al.* (2013)).

In this phenomenological description, no mention has been made to important issues that currently preclude further theoretical understanding of transcritical flows. The first one is the determination of critical values of pressure and temperature in mixtures, which may display quite disparate values from those of the separate components depending on the methods employed for their obtention (García-Córdova *et al.* 2011; Dahms & Oefelein

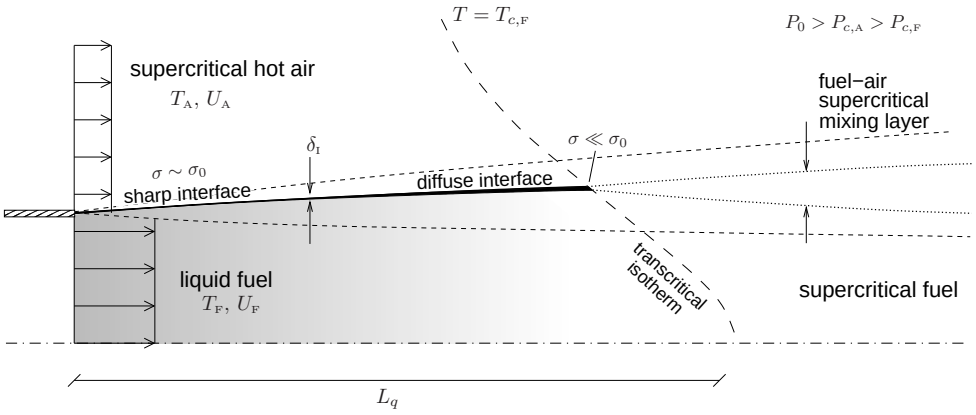

FIGURE 2. Schematic representation of the transcritical evolution of a liquid-fuel stream injected in a high-pressure combustion chamber. Initially, the interface separating the liquid and gas phases is of infinitesimal thickness (sharp). However, as heat is supplied to the jet from the surrounding gases, the interface grows in thickness (diffuse) until becoming a mixing layer downstream from the transcritical isotherm.

2013; Wensing *et al.* 2015; Qiu & Reitz 2015). The second one is the pyrolysis processes that hydrocarbon aviation fuels begin undergoing at temperatures of order 800 K, which are comparable to their critical temperatures (Edwards 2006). In particular, the cracking of the fuel may influence its physical properties near and beyond the critical temperature, including the surface tension. These, in turn, are open research questions that are beyond the scope of this report.

3. The diffuse-interface approach

The physical modeling of transcritical jet flows is challenging because of the requirement of having to simultaneously consider surface-tension effects and diffusive-mixing processes, as schematically shown in Figure 2. Near the orifice, the liquid and gas phases are separated by an infinitesimally thin interface, which exhibits discontinuous variations of physical properties and is endowed with surface tension forces while requiring a latent heat for vaporization. However, as heat is supplied to the liquid jet from the surrounding gas and the critical temperature is approached, the interface δ_I becomes thicker, the mean free path becomes smaller than δ_I, and the interfacial mechanisms of surface tension and latent heat of vaporization diminish. The diffuse-interface approach is based on the fact that the interface region enters the continuum range near the critical point, as described below.

The objective is to utilize the diffuse-interface approach to describe transcritical atomization by means of a single-fluid, multi-phase, multi-component formulation such that fuel and oxidizer species are described by their corresponding mass fractions Y_i regardless of their phase state, and are transported according to overall mixture conservation equations that treat the interfaces in the continuum range. For instance, consider the mass, momentum, total energy and species conservation equations

$$\frac{\partial \rho}{\partial t} + \frac{\partial}{\partial x_i}\left(\rho u_i\right) = 0, \tag{3.1}$$

$$\frac{\partial(\rho u_i)}{\partial t} + \frac{\partial}{\partial x_j}(\rho u_i u_j) = \frac{\partial \tau_{ij}}{\partial x_j} + \frac{\partial \mathcal{K}_{ij}}{\partial x_j}, \tag{3.2}$$

$$\frac{\partial(\rho e_t)}{\partial t} + \frac{\partial}{\partial x_i}(\rho u_i e_t) = -\frac{\partial q_i}{\partial x_i} - \frac{\partial \mathcal{Q}_i}{\partial x_i} + \frac{\partial}{\partial x_j}\left[(\tau_{ij} + \mathcal{K}_{ij})u_i\right], \tag{3.3}$$

$$\frac{\partial(\rho Y_k)}{\partial t} + \frac{\partial}{\partial x_i}(\rho u_i Y_k) = -\frac{\partial J_{i,k}}{\partial x_i} - \frac{\partial \mathcal{J}_{i,k}}{\partial x_i}, \tag{3.4}$$

where ρ is the mixture density, u_i is the mass-averaged velocity, τ_{ij} is the viscous stress tensor, q_i is the heat diffusion flux, $J_{i,k}$ is the molecular diffusion flux of species k, and e_t is the total energy. Additionally, $\mathcal{K}_{ij}$ is the capillary stress tensor (which includes pressure effects), and $\mathcal{Q}_i$ and $\mathcal{J}_{i,k}$ are, respectively, heat and mass fluxes caused by interfacial phenomena. The resulting formulation is expected to fail in regions below the critical point where the interfaces are not in the continuum range, while becoming equivalent to traditional descriptions of gaseous supercritical phenomena far above the critical point. In turbulent flows at high Reynolds numbers, the transcritical interfaces may be too small to be resolved numerically, yet the diffuse-interface approach provides a framework to filter the conservation equations and devise where interface-modeling closures are required.

Appropriate closures for $\mathcal{K}_{ij}$, $\mathcal{Q}_i$ and $\mathcal{J}_{i,k}$, along with an equation of state, must be provided in Eqs (3.2)-(3.4) that take into account the transcritical interface dynamics. Expressions for these quantities can be deduced from first principles, although the current developments are limited to single-component flows (Anderson *et al.* 1998) or binary mixtures (Papatzacos 2000). The methodology consists of obtaining first an expression for the entropy production resulting from the combination of mass, momentum, total energy, entropy and species conservation equations, with $\mathcal{K}_{ij}$, $\mathcal{Q}_i$ and $\mathcal{J}_{i,k}$ as unknown quantities. A set of expressions for these unclosed terms, based on constitutive assumptions and Onsager reciprocity relations, is then specified such that the entropy production is positive. As indicated below, the thermodynamic potentials involved in this process include the effects of interfacial inhomogeneities, which are also implicitly introduced in the equations of fluid motion through the definitions of the stress tensor and diffusion fluxes. A thermodynamically comprehensive development in this direction has been recently presented by Guo & Lin (2015).

The diffuse-interface closure problem described above is reviewed here in the context of single-component two-phase flows in absence of temperature gradients, where only $\mathcal{K}_{ij}$ needs to be determined, with further extensions to multi-component non-isothermal flows (such as those sketched in Figures 1(b,c) and 2) being deferred to future work.

3.1. *The van der Waals continuum-interface theory for single-component flows*

The theoretical foundations of the diffuse-interface approach were established by van der Waals (1893) more than one hundred years ago. The basis of the theory is that the region within the liquid-vapor equilibrium curve in the phase diagram is thermodynamically unstable, in that no stable thermodynamic state exists that describes a homogeneous mixture of liquid and vapor. Conversely, the theory predicts that the coexistence problem necessarily becomes singular with a thin interface separating both phases, and the Helmholtz free energy F depends on both the local and adjacent environment compositions. Assuming that the composition gradients are small compared to the reciprocal of the characteristic intermolecular distance, F can be approximated by a Taylor series expansion around the value of homogeneous bulk composition. In the first approximation,

and for an isotropic medium, the free energy of the interface is given by

$$F = \int_{\mathcal{V}} \left[\rho f + \frac{\kappa}{2} \left(\frac{\partial \rho}{\partial x_i} \frac{\partial \rho}{\partial x_i} \right) \right] d\mathcal{V}, \tag{3.5}$$

where $f = \int^{\rho} [P(\rho)/\rho^2] d\rho$ is the local specific free energy, with $P(\rho)$ the thermodynamic pressure obtained from an equation of state, $\mathcal{V}$ is the volume of integration enclosing the interface, and κ is a gradient energy coefficient. In particular, κ can be computed directly from kinetic-theory considerations of interactions between molecules in a density gradient (e.g. see Eq. (14) in Pismen (2001)), although most investigations utilize empirical correlations that make κ vanish above the critical temperature (Lin *et al.* 2007). Further details are given below in connection with surface-tension effects.

As first considered by Korteweg (1901), the condition of mechanical equilibrium for a two-phase system of a single-component fluid results in a second-order stress tensor that exemplifies the balance between pressure and surface-tension forces. The equilibrium conditions are obtained by searching the density profile across the interface that minimizes the free energy (3.5) subject to the mass-conservation constraint $\int_V (\rho - \rho_0)\, dV = 0$, where ρ_0 is an arbitrary constant that defines the amount of mass within the interface. A Lagrange multiplier μ, which plays the role of a generalized chemical potential, is employed to solve the corresponding minimization problem, which is equivalent to solving the Lagrange equation

$$\frac{\partial \mathcal{L}}{\partial \rho} - \frac{d}{dx_i} \left(\frac{\partial \mathcal{L}}{\partial (\partial \rho / \partial x_i)} \right) = 0, \tag{3.6}$$

where $\mathcal{L}$ is a Lagrangian given by

$$\mathcal{L} = \rho f + \frac{\kappa}{2} \frac{\partial \rho}{\partial x_i} \frac{\partial \rho}{\partial x_i} - \mu \rho, \tag{3.7}$$

with ρ and $\partial \rho / \partial x_i$ playing the role of generalized coordinates. In this way, the description of the density profile across the interface is obtained by substituting (3.7) into Eq. (3.6), which gives

$$\rho \kappa \frac{\partial^2 \rho}{\partial x_i \partial x_i} - \rho (f - \mu) - P = 0. \tag{3.8}$$

Variations of the gradient energy coefficient κ with ρ have been neglected in writing Eq. (3.8). The chemical potential μ, which is the same for both phases, is obtained by evaluating Eq. (3.8) far from the interface on the vapor (V) or liquid (L) sides,

$$\mu = \frac{\partial}{\partial \rho} (\rho f) \Big|_{V,L}. \tag{3.9}$$

For planar slender interfaces, Eq. (3.8) has a first integral of the form

$$\frac{1}{2} \kappa \left(\frac{d\rho}{dn} \right)^2 = \rho (f - \mu) + P_0, \tag{3.10}$$

subject to $\rho \to \rho_V$ at $n \to -\infty$, where P_0 is the pressure far from the interface, and n is a coordinate normal to the interface pointing into the liquid side. In particular, Eq. (3.10) corresponds to what is commonly referred to as gradient theory (Lin *et al.* 2007). A characteristic interface thickness δ_{I} can be estimated from Eq. (3.10) by linearizing the free energy around the critical point (Cahn & Hilliard 1958), which gives

$$\delta_{\text{I}} \sim (\rho_L - \rho_V) \sqrt{\frac{\kappa}{\rho_V R_g |T_c - T|}}. \tag{3.11}$$

It is worth mentioning that substitution of Eq. (3.10) into the one-dimensional version of Eq. (3.8) leads to

$$P - P_0 = \rho\kappa\frac{d^2\rho}{dn^2} - \frac{1}{2}\kappa\left(\frac{d\rho}{dn}\right)^2, \tag{3.12}$$

which describes the variations of disjoining pressure that warrant the mechanical integrity of the interface, with $P \to P_0$ at $n \to \pm\infty$. Such variations are, in turn, much smaller than P_0 near the critical point. Had interface curvature been included in deriving Eq. (3.10), a net pressure variation would occur across the interface as a result of capillary effects.

The Lagrange equation, Eq. (3.6), can be easily cast into the form (Goldstein 1980)

$$\frac{\partial \mathcal{K}_{ij}}{\partial x_j} = 0, \tag{3.13}$$

where

$$\mathcal{K}_{ij} = \mathcal{L}\delta_{ij} - \frac{\partial \mathcal{L}}{\partial(\partial\rho/\partial x_i)}\frac{\partial\rho}{\partial x_i} \tag{3.14}$$

is the corresponding stress tensor. In particular, upon substituting (3.7) into (3.14), the expression

$$\mathcal{K}_{ij} = -P\delta_{ij} + \rho\kappa\frac{\partial^2\rho}{\partial x_k\partial x_k} + \frac{1}{2}\kappa\left(\frac{\partial\rho}{\partial x_m}\frac{\partial\rho}{\partial x_m}\right)\delta_{ij} - \kappa\frac{\partial\rho}{\partial x_i}\frac{\partial\rho}{\partial x_j} \tag{3.15}$$

is obtained for the capillary stress tensor. It should be stressed here that condition (3.13) corresponds to mechanical equilibrium of the interface, as observed in Eq. (3.2). In a planar interface, the combination of Eqs. (3.14) and (3.15) is equivalent to Eq. (3.12).

Although the coefficient of surface tension does not appear explicitly in the formulation, surface-tension effects are volumetrically embedded in the stress tensor (3.15) through the density-gradient terms. Nonetheless, for a planar interface, an effective surface-tension coefficient can be defined as

$$\sigma = \kappa\int_{-\infty}^{+\infty}\left(\frac{d\rho}{dn}\right)^2 dn, \tag{3.16}$$

which accounts for the free energy accumulated in the density gradients. In the approach in which κ is calculated from correlations, an expression of the type

$$\ln\kappa = a_1 + a_2\ln\left(1 - \frac{T}{T_c}\right) + a_3\ln\left(1 - \frac{T}{T_c}\right)^2 \tag{3.17}$$

is used for $T/T_c < 0.95$, where the constants a_1, a_2 and a_3 are calibrated based on experimental measurements of the surface tension σ (Lin *et al.* 2007).

4. Conclusions and future work

A preliminary investigation of the modeling for atomization of liquid fuel jets at high-pressure transcritical conditions has been conducted. Based on scaling analyses, it is theorized that the ratio of the thermal-entrance length to the liquid-core length is an important hydrodynamic parameter that determines the overall relevance of transcritical dynamics in a high-pressure system. For instance, in operating conditions where the thermal-entrance length is much shorter than the liquid-core length, the liquid jet promptly becomes supercritical under no significant influence of surface-tension effects, as

in rocket-engine combustors where oxygen droplets are rarely observed. Conversely, when the thermal-entrance length is larger than the liquid-core length, the liquid jet breaks up before reaching supercritical conditions, with surface tension entering into the atomization dynamics. This last regime is encountered in high-pressure systems that employ non-preheated heavy hydrocarbon liquid fuels, such as gas turbines or internal combustion engines, in which large thermal-entrance lengths occur because of the relatively high critical temperatures involved.

The formulation of transcritical flows must describe the transition from subcritical regions where finite-thickness liquid-gas interfaces are subject to surface tension and latent heat of vaporization, to supercritical zones where surface-tension effects are negligible and molecular transport commands the gaseous mixing between fuel and air. However, the state of the art is based on formulations that model either subcritical or supercritical flows. The diffuse-interface approach shows potential to bridge both subcritical and supercritical regimes by considering the finite-thickness interface dynamics near the critical conditions. Nonetheless, most of the works performed to date using diffuse-interface are limited to single- or bi-component isothermal flows, and are oftentimes focused on mechanical equilibrium conditions as in the classic gradient theory. The broad potential of the diffuse-interface approach to render a single-fluid, two-phase multi-component set of conservation equations is likely a topic of interest for future research in this area.

Acknowledgments

This investigation was funded by AFOSR Grant # FA9550-15-C-0037.

REFERENCES

Anderson, D. M., McFadden, G. B. & Wheeler, A. A. 1998 Diffuse-interface methods in fluid mechanics. *Annu. Rev. Fluid Mech.* **30**, 139–165.

Banuti, D. T & Hannemann, K. 2014 Supercritical pseudo-boiling and its relevance for transcritical injection. *AIAA* Paper no. 2014-3571.

Cahn, J. W. & Hilliard, J. E. 1958 Free energy of a nonuniform system. I. Interfacial free energy. *J. Chem. Phys.* **28**, 258–267.

Crua, C., Manin, J. & Pickett, L. M. 2015 Transition from droplet evaporation to miscible mixing at diesel engine conditions. *13th Triennial International Conference on Liquid Atomization and Spray Systems ICLASS*.

Dahms, R. N., Manin, J., Pickett, L. M. & Oefelein, J. C. 2013 Understanding high-pressure gas-liquid interface phenomena in diesel engines. *Proc. Comb. Inst.* **34**, 1667–1675.

Dahms, R. N. & Oefelein, J. C. 2013 On the transition between two-phase and single-phase interface dynamics in multicomponent fluids at supercritical pressures. *Phys. Fluids* **25**, 092103.

Edwards, T. 2006 Cracking and deposition behavior of supercritical aviation fuels. *Combust. Sci. Tech.* **178**, 307–334.

García-Córdova, T., Justo-García, D. N., García-Flores, B. E. & García-Sánchez, F. 2011 Vapor-liquid equilibrium data for the nitrogen-dodecane system at temperatures from 344 to 593 K and at pressures up to 60 MPa. *J. Chem. Eng. Data* **56**, 1555–1564.

Goldstein, H. 1980 *Classical mechanics*. Addison-Wesley.

Gorokhovski, M. & Herrmann, M. 2008 Modeling primary atomization. *Annu. Rev. Fluid Mech.* **40**, 343–366.

Guo, Z. & Lin, P. 2015 A thermodynamically consistent phase-field model for two-phase flows with thermocapillary effects. *J. Fluid Mech.* **766**, 226–271.

Korteweg, D. J. 1901 Sur la forme que prennent les équations du mouvement des fluides si l'on tient compte des forces capillaires causées par des variations de densité considérables mais continues et sur la théorie de la capillarité dans l'hypothese d'une variation continue de la densité. *Arch. Néerl. Sci. Exactes Nat. Ser. II* **6**, 1–24.

Lasheras, J. C & Hopfinger, E. J. 2000 Liquid jet instability and atomization. *Annu. Rev. Fluid Mech.* **32**, 275–308.

Lin, H., Duan, Y.-Y. & Min, Q. 2007 Gradient theory modeling of surface tension for pure fluids and binary mixtures. *Fluid Phase Equilib.* **254**, 75–90.

Mayer, W. O. H., Ivancic, B., Schik, A. & Hornung, U. 2001 Propellant atomization and ignition phenomena in liquid oxygen/gaseous hydrogen rocket combustors. *J. Propulsion Power* **17**, 794–799.

Mongia, H. C 2013 N+3 and N+4 generation aeropropulsion engine combustors: Part 6: Operating Conditions, target goals and lifted jet. *AIAA* Paper no. 2013-3654.

Papatzacos, P. 2000 Diffuse-interface models for two-phase flow. *Physica Scripta* **61**, 349–360.

Pismen, L. M. 2001 Nonlocal diffuse interface theory of thin films and the moving contact line. *Phys. Rev. E* **64**, 021603.

Qiu, L. & Reitz, R. D. 2015 An investigation of thermodynamic states during high-pressure fuel injection using equilibrium thermodynamics. *Int. J. Multiphase Flow* **72**, 24–38.

Sánchez, A. L., Urzay, J. & Liñán, A. 2014 The role of separation of scales in the description of spray combustion. *Proc. Comb. Inst.* **35**, 1549–1577.

Segal, C. & Polikhov, S. A. 2008 Subcritical to supercritical mixing. *Phys. Fluids* **20**, 052101.

Sirignano, W. A. 2010 *Fluid Dynamics and Transport of Droplets and Sprays.* Cambridge Univ. Press.

Sirignano, W. A. & Delplanque, J. P. 1999 Transcritical vaporization of liquid fuels and propellants. *J. Propulsion Power* **15**, 806–902.

van der Waals, J. D. 1893 The thermodynamic theory of capillarity under the hypothesis of a continuous variation of density. Translated by J. S. Rowlinson in *J. Stat. Phys.* **20**, 197–244, 1979.

Wensing, M., Vogel, T. & Götz, G. 2015 Transition of diesel spray to a supercritical state under engine conditions. *Int. J. Engine Res.* **17**, 108–119.

Yang, V. 2010 Modeling of supercritical vaporization, mixing, and combustion processes in liquid-fueled propulsion systems. *Proc. Comb. Inst.* **28**, 925–942.

Yu, J. & Eser, S. 1995 Determination of critical properties of some jet fuels. *Ind. Eng. Chem. Res.* **34**, 404–409.